Integrating physical and genetic signals for programming across time scales in the mammalian cell.

Alexandre R. Sathler*
*UC Berkeley / UC San Francisco Joint Graduate Program in Bioengineering
Submitted to Principles of Synthetic Biology (Fall 2025)

Increasingly complex biological circuits designed by synthetic biologists necessitate robust signal delay machinery for connections across time scales. Here, I present TRAM: a synthesis of engineered protease cascades and cellular trafficking for a novel, programmable, minutes-scale signal delay mechanism for use in biological circuits.

Trafficking | Protease Cascades | Signal Delays

1 Introduction

While modern biological circuit design increasingly enables tight control of signal response behavior (Brophy & Voigt, 2014), synthetic signal response delays present significant challenges. Traditionally, response delays are either engineered via nested transcriptional gating or altered protein stability.

Nested transcriptional gates provide broad design space for signal delays, but mismatched gate dynamic ranges combine with transcription-al stochasticity variability to attenuate output (Fig 1a). One alternative prolongs biological signals through physical persistence of signaling proteins (Weber et. al, 2007; Koh et. al, 2009; Wauford et. al, 2024), but utility is limited by the epigenetic silencing of long-lasting proteins in mammalian systems (Kim et. al, 2011). Persistent proteins also necessitate symmetrical ON and OFF kinetics: while long delays between ON and OFF signals may be achieved, signal periodicity is sacrificed (Fig. 1b).

Here, I model a novel delay mechanism combining protease cascades (Stein & Alexandrov, 2014; Yang et. al, 2025) with endogenous cellular **tra**nsport **m**achinery (TRAM) to achieve tunable stepwise delays between ON and OFF signals for idealized delays kinetics (Fig 1c.). To validate TRAM utility for synthetic biology, I demonstrate its superiority over traditional methods in producing a tunable, lightly attenuated output delay in response to pulsatile optogenetic stimulation.

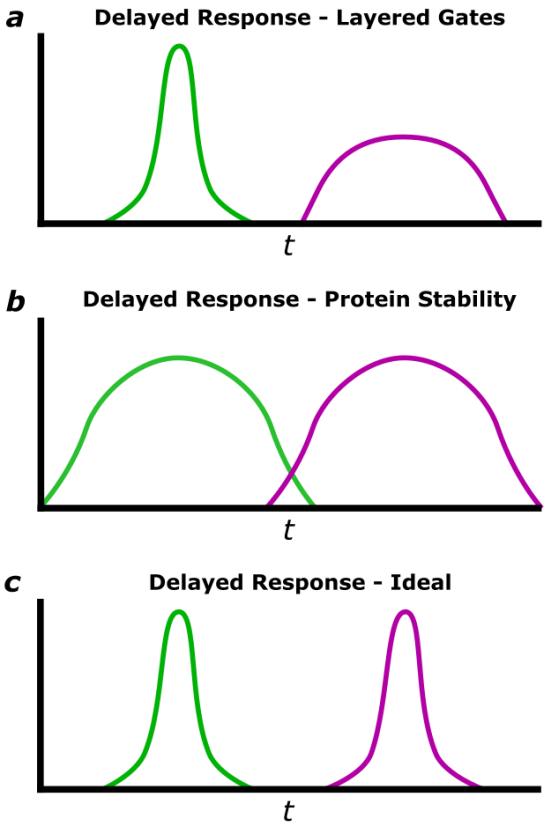

2 TRAM Mechanism

As modeled, TRAM trafficking is induced by the addition of modular TRAM domains to a transcription factor (TF). Each TRAM domain consists of a nuclear localization sequence (NLS) and mitochondrial localization sequence (MTS) separated by an orthogonal protease cleavage site The identity of the localization domain terminal to the transcription factor (NLS or MTS) induces trafficking and subsequent proteolytic cleavage (Fig 2).

To enable robust trafficking and cleavage, orthogonal TEV and TVMV proteases are constitutively expressed (Renna et. al, 2022). along with NLS or MTS ligand-binding sites at the membrane of respective sub-cellular organelles. Constitutive expression of these machinery

leverages the endogenous mitochondrial outer-membrane protein 20 (Tom20) membrane localization mechanism, where Tom20 transmembrane domains are recognized by mitochondrial inner-membrane protein 1 (Mim1) and inserted into the membrane.

After TF-TRAM construct expression, TF activity is delayed by sequential rounds of TRAM-mediated subcellular trafficking and TEV/TVMV-mediated proteolytic cleavage (Fig. 2a-c). The following is an example TF-TRAM construct with three TRAM domains:

TF-Ubr1-TVMV$_1$-NLS$_1$-TEV$_1$-MLS$_1$-TVMV$_2$-NLS$_2$-TEV$_2$-MLS$_2$-TVMV$_3$-NLS$_3$-TEV$_3$-MLS$_3$

The construct also contains Ubr1, a degron tag that ensures fast degradation (Varshavsky, 2019) upon TRAM domain exhaustion and TF localization to the nucleus (Fig. 2d).

3 Methods

To focus on circuit-level behavior as opposed to the complexities of biochemical implementation, I make four simplifying assumptions:

I. *Only the outermost cellular localization sequence is recognized*. Ensures sequential TRAM domain cleavage.

II. *Only the outermost protease cleavage site is accessible*. N-terminal protease cleavage sites are too distal from the protease for activity.

III. *The TF cannot enter the nucleus until all TRAM domains have been removed*. Ensures cleaves of all TRAM domains.

IV. *The Ubr1 domain is only active after all TRAM domains have been removed.* TF-TRAM construct persistence in the cytosol until all TRAM domains have been removed.

These principles protein engineering and biochemical implementation for the future, allowing this work to focus on evaluating the merits of subcellular transcription factor trafficking for time-delay circuits in synthetic biology. I model TRAM delays as sequential trafficking between nucleus and mitochondria, with each cycle adding predictable delay and enabling sequential trafficking and proteolytic cleavage.

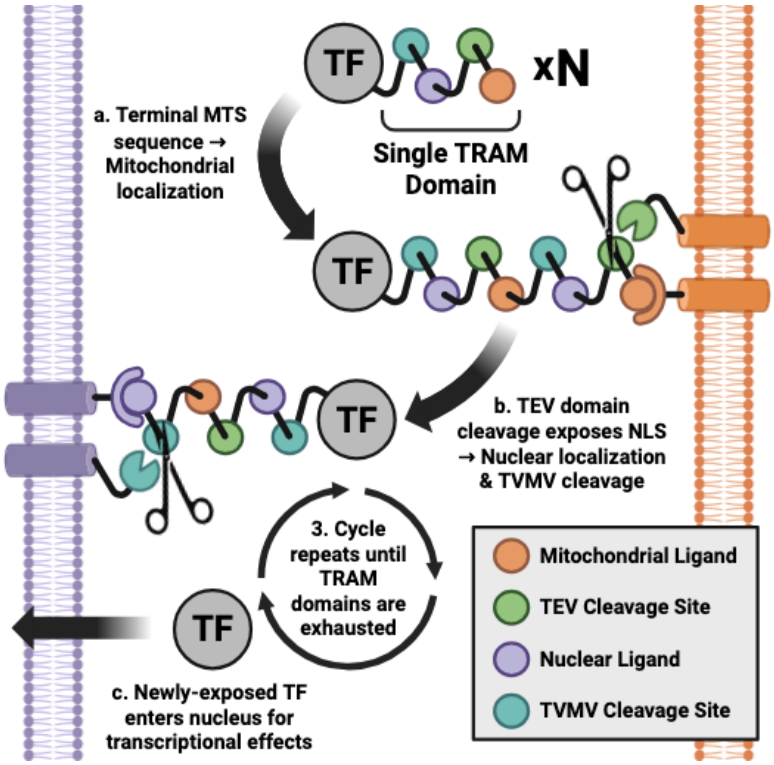

Figure 2: Schematic of TRAM Trafficking. TRAM is a tunable, physically separated sequential protease pathway. **a,** Terminal MTS sequences induce trafficking to the mitochondrial membrane, where MTS ligand-binding brings TF-TRAM constructs proximal to membrane-localized TEV protease **b,** TEV mediated proteolytic cleavage exposes NLS sequence (now terminal), inducing nuclear membrane trafficking. A mirrored NLS ligand-binding event localizes the TF-TRAM construct nearby to membrane-localized TVMV protease. **c,** TVMV mediated proteolytic cleavage reveals underlying TRAM domains if they are present, inducing another cycle of trafficking and TEV/TVMV cleavage. **d,** Upon exhaustion of all TRAM domains, the TF-Ubr1 construct is exposed and trafficked into the nucleus for transcriptional modulation and degradation.

3.1 Basic TRAM Model

I model TRAM delays as sequential trafficking between nucleus and mitochondria, with each cycle adding predictable delay and enabling sequential trafficking and proteolytic cleavage.

$$TFn_n \rightarrow TFn_m \rightarrow TFnC_m \rightarrow TFnC_n \rightarrow TF(n-1)_n \rightarrow \cdots \rightarrow TF \quad (0)$$

For definitions, see Supplementary Table 2. In compositor form, each trafficking and proteolytic processing step is converted into an ordinary differential equation (ODE):

$$\frac{dTFn_n}{dt} = k_{tx}PROM - \frac{V_a}{R_m}TFn_n - k_{dTR}TFn_n \quad (1.1)$$

$$\frac{dTFn_m}{dt} = \frac{V_a}{R_m}TFn_n - k_{TE}TFn_m - k_{dTR}TFn_m \quad (1.2)$$

$$\frac{dTFnC_m}{dt} = k_{TE}TFn_m - \frac{V_a}{R_m}TFnC_m - k_{dTR}TFnC_m \quad (1.3)$$

$$\frac{dTFnC_n}{dt} = \frac{V_a}{R_m}TFnC_m - k_{TV}TFnC_n - k_{dTR}TFnC_n \quad (1.4)$$

$$\frac{dTF(n-1)_n}{dt} = k_{TV}TFnC_n - \frac{V_a}{R_m}TF(n-1)_n - k_{dTR}TF(n-1)C_n \quad (2.1)$$

... (2-N)

$$\frac{dTF}{dt} = k_{TV}TF1C_n - k_{dTF}TF1C_n \quad (N.4)$$

Above, the fifth equation was written to illustrate the cyclical nature of the described ODE system: when the final TRAM domain component is cleaved from the previous cycle, the next cycle begins. The final equation depicts the final step where the final TRAM domain is cleaved and TF-Ubr1 becomes transcriptionally active.

3.2 Input Pulse Modeling

4 Results

4.1 Short input pulses are required for scale-appropriate TRAM delays.

I first modeled a TF-TRAM construct with four TRAM domains (TF-4xTRAM) using system parameters consistent with empirically-measured values of underlying biological phenomena (Supp. Table 1). The initial TF-4xTRAM construct was produced via a transcriptional pulse lasting three hours (CITATION), and output TF concentrations were graphed with respect to time (Fig. 1a). While a relative expression unit (REU) output delay was observed, its timing was indistinguishable from that of trafficking intermediates, suggesting that any delay observed resulted from transcriptional dynamics as opposed to TRAM trafficking.

I then wondered whether a shorter TF-TRAM transcriptional pulse would resolve incremental time delays associated with trafficking of individual TRAM domains. I modeled a six-minute, optogenetically-induced pulse (CITATION) of transcriptional activity of the same TF-4xTRAM construct. Output TF expression was delayed relative to the initial pulse and residual expression of TRAM intermediates were resolved (Fig. 1b) unlike the transcriptional pulse.

4.2 Output signal delays scale linearly with TRAM domain count.

To investigate whether incrementally appending TRAM domains to the TF-TRAM construct would incrementally increase output signal delays, I modeled TF-TRAM constructs with between one and eight TRAM domains. Encouragingly, each additional TRAM domain incrementally increased output delays when initially induced by an optogenetic pulse (Fig. 1c). This was confirmed via regression analysis, which produced a perfect linear fit to increasing time delays (Fig. 1d). A perfect logarithmic fit of output peak REU indicates that additional TRAM domains also attenuate signal (Fig. 1e), which is an inherent characteristic of protein degradation rates in the cytosol. These results suggest that each additional TRAM domain adds 140 seconds of delay between input and output signals under literature-informed conditions.

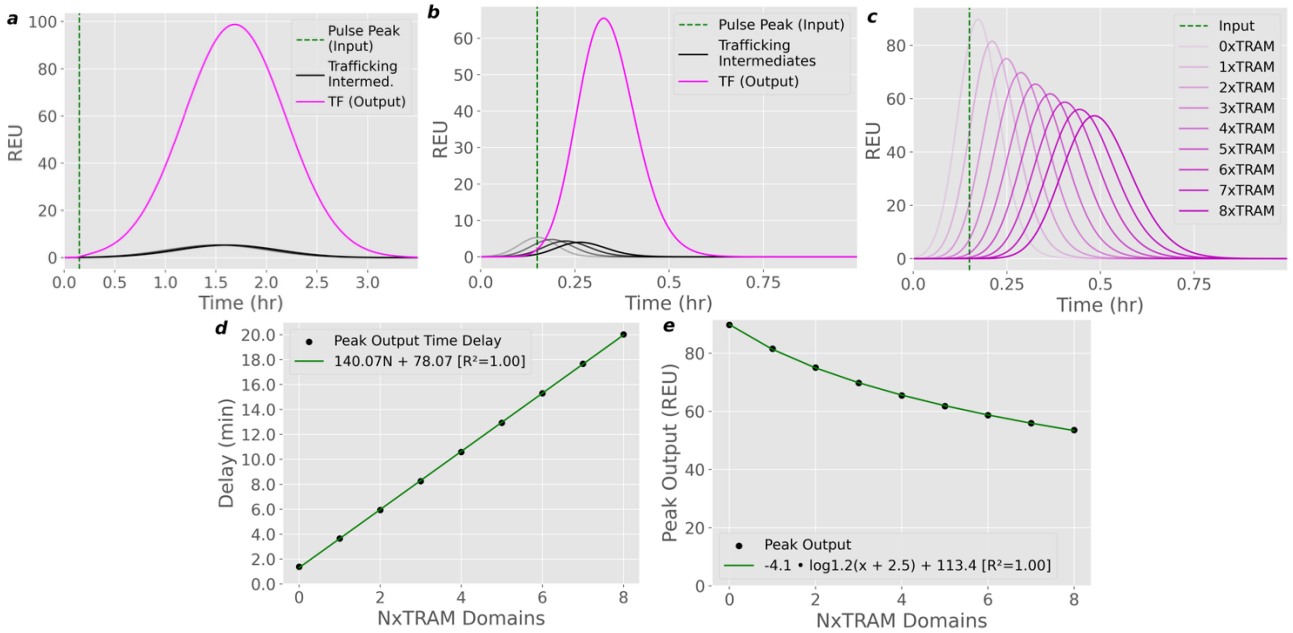

Figure 3 | Effect of Pulse Duration and TRAM Domains on Output Delay. Depictions of output signal peaks based on a simulated TF-TRAM system. **a**, Model with parameters rigidly faithful to biological plausibility, TF-4xTRAM output signal is significantly delayed from peak input signal, but intermediate trafficking is not resolved. **b,** A short optogenetic pulse resolves TRAM intermediates in the TF-4xTRAM construct. **c,** Incrementally adding TRAM domains to TF-TRAM construct increases output time delay. **d,** Signal delay scales linearly with TRAM domain count. **e,** Output signal amplitude decreases logarithmically with increasing TRAM domain count.

4.3 Characterizing TRAM delay behavior in system parameter space.

5 TRAM System Dynamics in Parameter Space

6 TRAM vs. Gate Layering in Synthetic Circuits

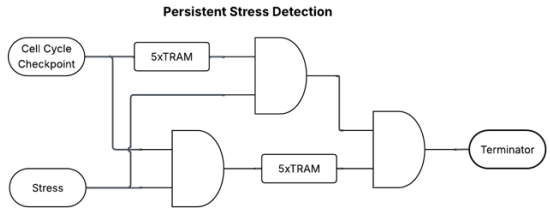

7 Citations

Brophy, J., Voigt, C. Principles of genetic circuit design. *Nat Methods* **11**, 508–520 (2014). doi.

Das, S., Vera, M., Gandin, V., Singer R.H., Tutucci E. Intracellular mRNA transport and localized translation. *Nature Reviews Molecular & Cell Biology* **22**, 483–504 (2021). Doi.

Hulett, J.M., Lueder, F., Chan, N.C., Perry, A.J., Wolynec, P., Likić, V.A., Gooley, P.R., Lithgow, T. The transmembrane segment of Tom20 is recognized by Mim1 for docking to the mitochondrial TOM complex. *J Mol Biol.* **376**(3), 694-704 (2008). doi.

Kim, M., O'Callaghan, P. M., Droms, K. A. & James, D. C. A mechanistic understanding of production instability in CHO cell lines expressing recombinant monoclonal antibodies. *Biotechnol. Bioeng.* **108**, 2434–2446 (2011). doi.

Koh, K.W., Lehming, N., Seah, G.T. Degradation-resistant protein domains limit host cell processing and immune detection of mycobacteria. *Mol Immunol* **46**, 1312-1318 (2009). doi.

Li, J., Wu, F., Cheng, L., Zhang, J., Cha, C., Chen, L., Feng, T., Zhang, J., Guo, G. A nuclear localization signal is required for the nuclear translocation of Fign and its microtubule-severing function. *Mol Med Rep.* **21**(6), 2367-2374 (2020). doi.

Renna, P., Ripoli, C., Dagliyan, O., Pastore, F., Rinaudo, M., Re, A., Paciello, F., Grassi, C. Engineering a switchable single-chain TEV protease to control protein maturation in living neurons. *Bioeng Transl Med.* **7**(2), e10292 (2022). doi.

Stein, V., Alexandrov, K. Protease-based synthetic sensing and signal amplification, *Proc. Natl. Acad. Sci. U.S.A.* **111** (45), 15934-15939 (2014). doi.

Varshavsky, A. N-degron and C-degron pathways of protein degradation, *Proc. Natl. Acad. Sci. U.S.A.* **116** (2) 358-366 (2019). doi.

Wauford, N., Wachter, G., Kiwimagi, K., Weiss, R. A Tunable Long Duration Pulse Generation Circuit in Mammalian Cells. *ACS Synthetic Biology* 13, 11, 3576–3586 (2024). doi.

Weber, W., Stelling, J., Rimann, M., Keller, B., Daoud-El Baba, M., Weber, C.C., Aubel, D., Fussenegger, M. A synthetic time-delay circuit in mammalian cells and mice, *Proc. Natl. Acad. Sci. U.S.A.* **104** (8) 2643-2648 (2007). doi.

Yang, H.K., Muthukumar, P.K., Chen, W. Synthetic protein degradation circuits using programmable cleavage and ligation by Sortase A. *Nat Commun.* **16**(1), 8682 (2025). doi.

8 Supplemental Information

***Table 1*:** Biophysical modeling parameters		
Variable	**Description**	**Value**
R_n	Mean radius of the nucleus	2.5μm
R_c	Mean radius of a cell	7.5μm
R_m	Mean nucleus-mitochondria distance	2.5μm
V_a	Velocity of motor protein trafficking	0.47μm/s
V_d	Linear diffusion coefficient in cytoplasm	27μm^2/s

***Table 2*:** Parts in a single TRAM trafficking cycle	
Variable	**Description**
TFn_n	TF with *n* TRAM domains localized at the nucleus.
TFn_m	TF with *n* TRAM domains localized at the mitochondria.
$TFnC_m$	TF with *n* TRAM domains localized at the mitochondria, after TEV cleavage.
$TFnC_n$	TF with *n* TRAM, post-TEV cleavage, re-localized to the nucleus.
$TF(n\text{-}1)_n$	TF, post-TVMV cleavage, now containing *n-1* TRAM domains
TF	TF-Ubr1 free of TRAM domains that traffics to nucleus for transcriptional modulation and degradation